Parametric Evaluation of Web Offset Fluting

Steve Simmons*, Bruce Blom*[§], Chris Dreher**, Dean Dewildt***, Doug Coffin**

Keywords: Fluting, Web Offset, Hygroexpansivity, Corrugations

Abstract: Fluting is a ubiquitous problem of the web offset printing process. Flutes, or corrugations, are seen as ridges, running parallel to the web direction, that have a characteristic wavelength of from 15 to 30 millimeters. They are found only in regions of heavy ink coverage. The concept that these are due to differential shrinkage in the cross-direction (CD) of the web is explored and coating variables examined to determine their influence on the wavelength and amplitude of the flutes.

Background

Flutes are MD-oriented corrugations present in heavily inked regions of web heatset-printed paper. The flutes generally have a characteristic wavelength and amplitude, as depicted in Figure 1. MacPhee, *et al.* (2000) have recently reviewed the literature on web offset fluting. That work, part of an industry-wide initiative, sought to identify pressroom factors that affected the severity of the problem. In the process they validated the model proposed by Hirabayashi *et al.* (1998) that concluded that the origin of flutes was due to differential shrinkage, in the cross direction of the web, between areas of heavy ink coverage and area of no coverage. In essence, the ink acts as a barrier to moisture loss from within

* Mead Corporation
** Institute of Paper Science and Technology
*** Dow Chemical
§ To whom correspondence should be addressed – BEB1@mead.com

Figure 1. Flute Nomenclature (after MacPhee, *et al.* (2000)

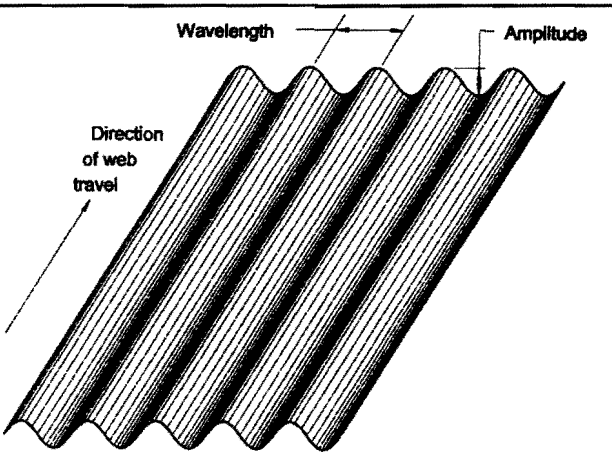

the sheet as it passes through the web oven, so that the inked area does not lose moisture as quickly as the non-inked region. Paper fibers shrink much more in their diameter than in their length, as they are dried. Consequently, because the fibers are preferentially aligned in the machine direction, web shrinkage occurs in the cross direction, or CD – see Figure 2.

Figure 2. Origin of Flutes

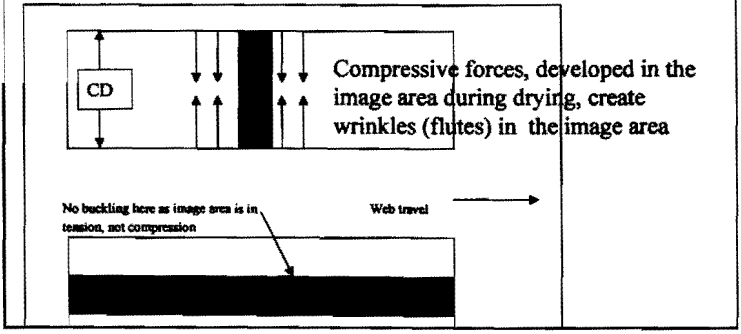

Among the findings clearly demonstrated in the MacPhee (*ibid.*) report are as follow:

- It is the moisture contained within the paper itself that controls the shrinkage. Moisture applied by the dampening system does not contribute to the phenomenon.
- Post-oven moisture levels are indeed lower in the non-image areas compared with the imaged areas.
- The presence of an overprint varnish, in the non-image area, reduces the severity of fluting – this is consistent with the concept that the varnish acts as a barrier, just like the ink, in retarding moisture loss.
- Web tension, over the range that can typically be applied on press, has no effect on the severity of the flutes. A minimum tension is required to establish the characteristic orientation of the flutes, however.
- Web operating conditions – oven temperature and press speed had little effect on the severity of the flutes

Experimental

The purpose of the work to be described was to identify what coated paper properties, particularly with respect to the coating, might affect the severity of fluting.

A coating experiment was designed to look at component variations that are thought to contribute to differences in the coated paper stiffness. Three independent coating variables were explored:

* Kaolin Clay to Ground Calcium Carbonate Ratio (CLAY/CaCO3)
* S/B Latex to Ethylated Starch Ratio (LATEX/STARCH)
* T_g of the Latex (LATEX T_g)

Formulations are shown in Table 1. Each coating was formulated and lab coated on a 63 lb/ 3300 sq. ft. woodfree raw stock. Approximately 7.5 pounds of coat weight were applied to both sides making an 80# finish sheet. The finished papers received light (1 nip) lab calendering.

The dynamic mechanical properties of the latex films, latex/starch films, coating films, and coated paper in the linear viscoelastic regime were determined using a Rheometrics RSA II instrument at 1 rad/sec from -30 deg C to 100 deg C. The latex films, latex/starch films, and coatings were evaluated using a shear stress test which yields the shear modulus (G') over a range of temperatures. The coated paper was evaluated in both machine and cross machine directions using a tensile stress test which yields Young's modulus (E') over the range of temperatures.

Table 1. Coating Compostions

Sample #	Clay / CaCO3, %	Latex / Starch, Parts	Latex T_g, °C	Designation
1	100/0	8/8	9	100/0, 8/8, T_g=9
2	75/25	8/8	9	75/25, 8/8, T_g=9
3	50/50	8/8	9	50/50, 8/8, T_g=9
4	25/75	8/8	9	25/75, 8/8, T_g=9
5	0/100	8/8	9	0/100, 8/8, T_g=9
6	50/50	0/16	9	50/50, 0/16, T_g=9
7	50/50	4/12	9	50/50, 4/12, T_g=9
8	50/50	12/4	9	50/50, 12/4, T_g=9
9	50/50	16/0	9	50/50, 16/0, T_g=9
10	50/50	12/4	25	50/50, 12/4, T_g=25
11	50/50	12/4	-30	50/50, 12/4, T_g=-30

The latex and latex/starch films were prepared as follows. Three-inch diameter Teflon O-rings were taped onto a flat Teflon surface. The temperature of the Teflon surface was maintained between 35 and 40 deg C. Sufficient latex was poured into the area defined by the O-ring. Care was taken to exclude air bubbles. When the samples were dried, they were removed from the Teflon surface. The samples were dried further in a forced-air oven at 80 deg C until completely dry. Samples of 1-2 mm thickness were obtained.

The coatings were prepared by drawing them down on polyester film using a #14 Meyer rod. The coatings were then dried in a forced air oven at 120 deg C for 2 minutes. After the coating films had equilibrated to room temperature, they were removed from the polyester film. The freestanding films were then cut into 1/4 inch strips.

To prepare the coated paper samples, ¼-inch wide strips of the coated paper were cut in both the MD and CD.

Full size rolls were also produced using the MCR #11 Pilot Coater. The same coatings used for the lab testing were applied at 7.5#/side to the same base sheet. Calendering conditions were held constant for all coating variations.

Trial papers were subsequently printed on a commercial scale web offset press at RIT. Two oven temperatures were employed (270 and 320 degrees F) and oven dwell time was varied from 2 to 4 seconds by changing press speed (1000 to 500 fpm). A common form was used for all conditions, with particular emphasis on a solid black (200%/200%) region of prescribed aspect ratio. The fluting produced in this printed region was characterized by wavelength and amplitude as determined by Fourier analysis of scanning laser profilometry data representing each trial case. Fluting amplitudes and wavelengths were generally consistent with expectations based on prior data. Note that profilometry data were collected several weeks after testing and represent the flutes in their "relaxed state (Mochizuki (1981)).

Results

Thermal Studies

Only the effects of the Kaolin Clay to Ground Calcium Carbonate Ratio (CLAY/CaCO3) and the Ethylated Starch Ratio to S/B Latex (STARCH/LATEX) on the coating films and CD direction of the paper will be reported on here.

Coating Films

Figure 3 shows the influence different clay to carbonate ratios have on the modulus of coating films.

Clay is typically thought to impart more stiffness than carbonate, likely because of its more plate-like morphology. This DMS testing indicated that this theory was only valid at higher temperatures (>30°C). 100 percent carbonate had the lowest moduli at all temperatures. At lower temperatures, the 75/25 clay/$CaCO_3$ blend had the highest moduli, followed by 50/50 and 25/75 blends, respectively. While these results appear unexpected, previous work done at Dow, shows similar re sults. These unexpected results are likely due to different packing efficiencies of the pigments, and hence, different coating porosities. Higher coating porosity would result in lower modulus coatings.

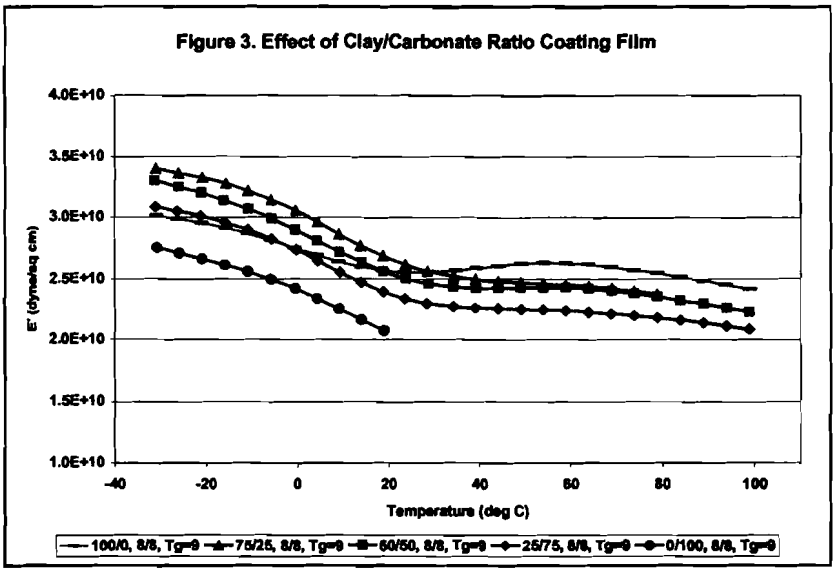

Figure 4 is the effect of different starch to latex ratios on coating films. From the starch/latex film results, we would anticipate higher starch levels would translate to higher moduli at high temperatures, but what we see from this data is that 8/8 and 12/4 ratios have higher moduli than the 16/0 ratio. A likely explanation for this is the fact that starch will impart more porosity to a dried paper coating than latex. Again, the additional air in the all starch coatings may more than offset increases due to the stiffer material.

CD Direction Paper

With respect to clay/carbonate ratios, Figure 5, generally higher clay levels meant higher moduli; however, this statement was really only pronounced in the all carbonate sample.

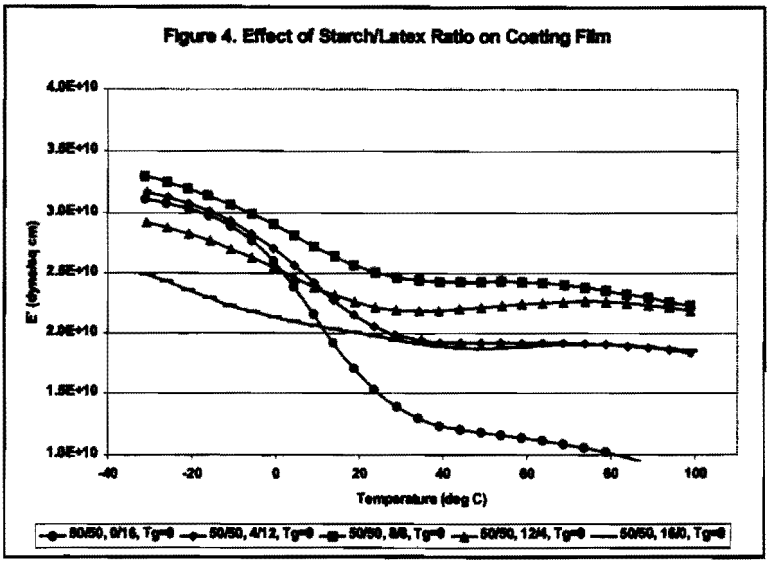
Figure 4. Effect of Starch/Latex Ratio on Coating Film
4.0E+10
3.5E+10
3.0E+10
2.5E+10
2.0E+10
1.5E+10
1.0E+10
E' (dynes/sq cm)
-40
-20
0
20
40
60
80
100
Temperature (deg C)
80/50, 0/16, Tg=0
50/50, 4/12, Tg=0
50/50, 8/8, Tg=0
50/50, 12/4, Tg=0
50/50, 16/0, Tg=0

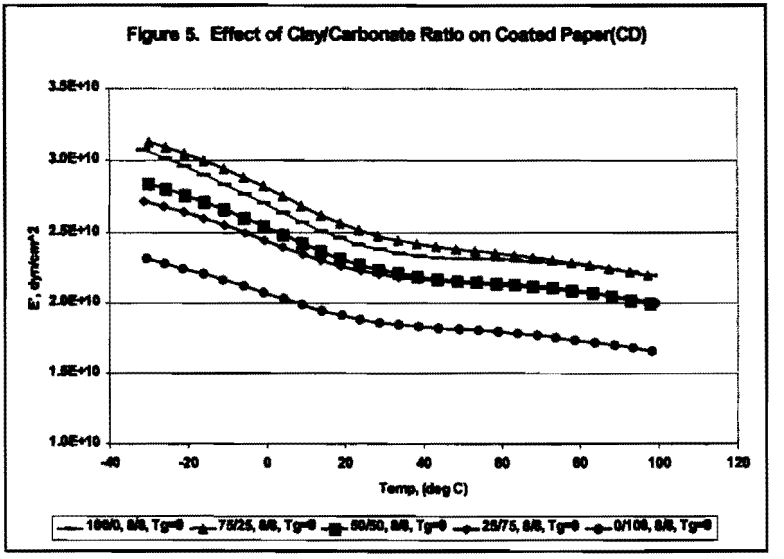
Figure 5. Effect of Clay/Carbonate Ratio on Coated Paper(CD)
3.5E+10
3.0E+10
2.5E+10
2.0E+10
1.5E+10
1.0E+10
E', dyn/cm^2
-40
-20
0
20
40
60
80
100
120
Temp, (deg C)
100/0, 8/8, Tg=0
75/25, 8/8, Tg=0
50/50, 8/8, Tg=0
25/75, 8/8, Tg=0
0/100, 8/8, Tg=0

Figure 6. Effect of Starch/Latex Ratio on Coated Paper(CD)

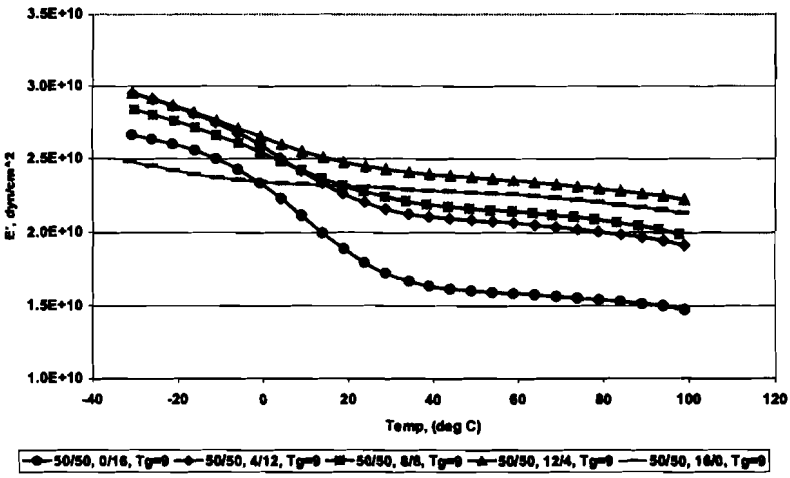

As for starch/latex ratios, Figure 6, typically higher starch levels resulted in higher moduli, but the all starch formulations were not the highest. Typically, a 4/12 blend of starch /latex resulted in the highest modulus followed by 8/8. Even in the coated paper, we can see how the starch/latex ratio in the coating of that finished paper sample can influence the viscoelastic properties.

From previous work done to improve coated paper stiffness with stiffer coatings and latexes, we would have anticipated that higher clay/carbonate ratio, lower latex/starch ratio, and higher latex T_g would increase the moduli of coated paper. This study suggests that these presumptions are correct, except that the particular high T_g latex (25°C) used resulted in lower moduli for the coatings and paper. Also unexpectedly, all-clay pigment systems or all-starch binder systems did not provide the highest moduli when looking at pure coating films. Both of these unexpected phenomena might be explained by likely increases in coating porosity due to less film formation in the case of the binders, and lower particle packing efficiencies in the case of the pigments.

Press Results

Figures 7 and 9 show the amplitude and wavelength data determined for each trial paper under each print trial condition. Figure 11 provides an estimate of differential shrinkage (between imaged and non-imaged areas), which may be computed for each case from the amplitude-wavelength pairs. Note that the central point in the clay to carbonate series is identical to the central point in the

Figure 7. Fluting Amplitudes by Condition (web exit temperature and oven dwell time)

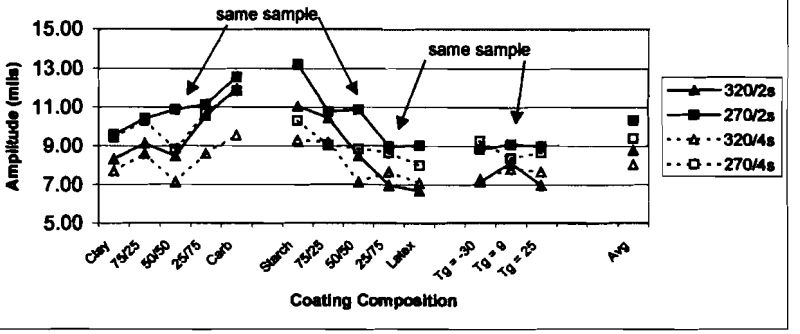

Figure 8. Fluting Amplitudes - Typical (web exit temperature and oven dwell time)

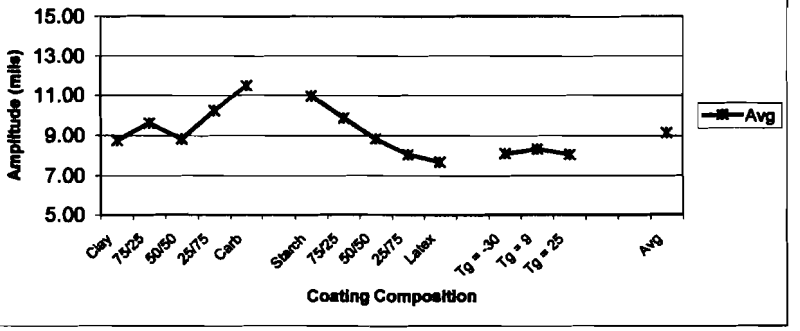

Figure 9. Fluting Wavelength by Condition web exit temperature/oven dwell time

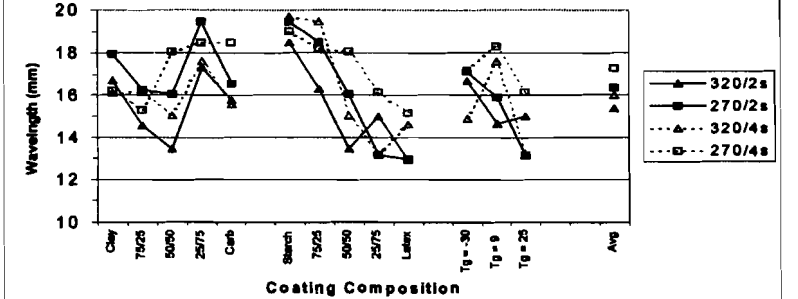

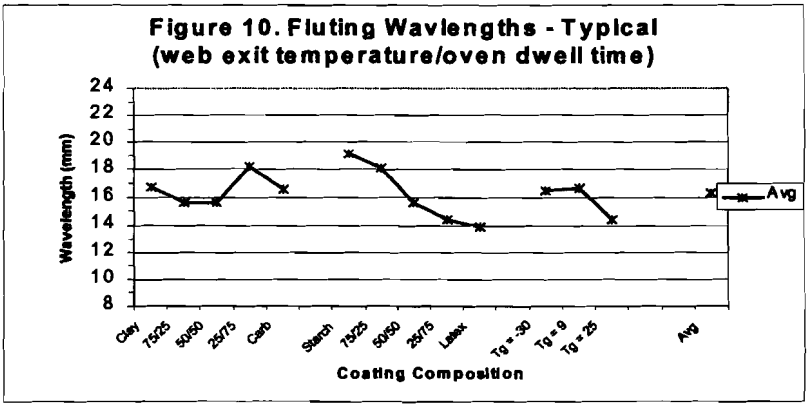

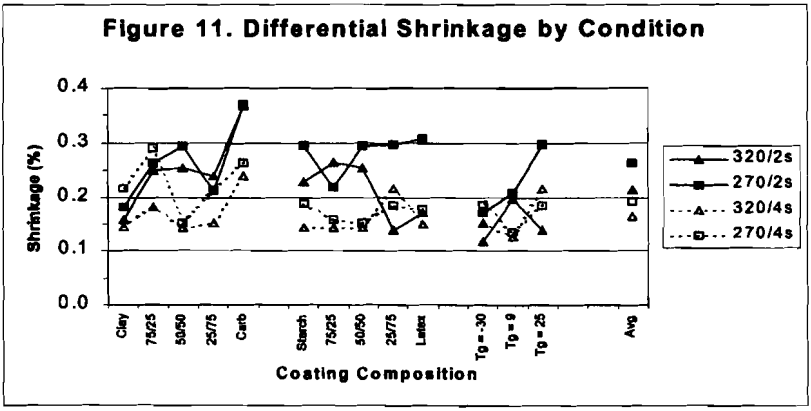

starch to latex series, as this point represents a single coating formulation condition. Similarly, the central point in the latex series is identical to the fourth point in the starch to latex series – again this represents a single coating formulation condition. Finally, Figures 8-12 reproduce Figures 7 through 11, but represent averaged values for each trial coating.

Several trends are readily apparent in the presented data. Variations in amplitude are greater than variations in wavelength, and appear more sensitive to drying conditions. In fact, the data indicate that increased drying on press decreases fluting amplitude (low oven temperature/short dwell time yields maximum flute amplitudes – increasing oven temperature and dwell time yields minimum amplitudes). Increasing carbonate or starch level increases the amplitude of measured flutes. Increasing starch level also decreases the number of flutes (increases wavelength), while increasing carbonate does not provide this

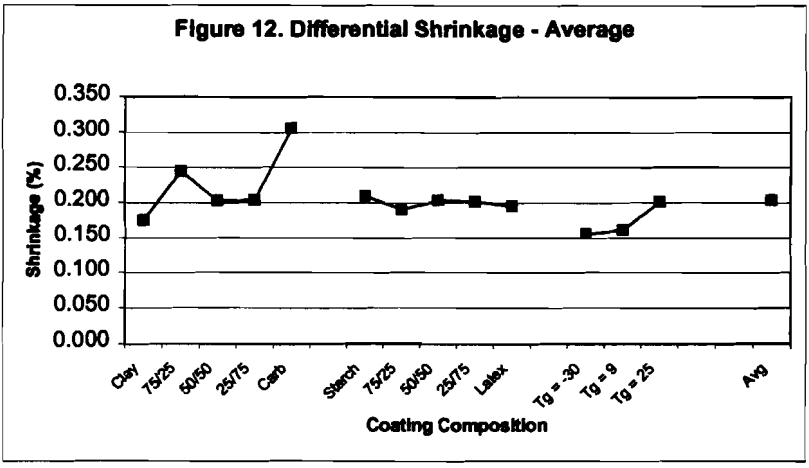

effect. Accordingly, increasing carbonate level may increase the differential shrinkage, while the binder type plays no apparent role in differential shrinkage. Finally, latex type has a greater influence on wavelength than amplitude of measured flutes.

Discussion

Discussion of Variables

Resolving the various trends presented in the data requires reconciliation of several potentially competing effects. An analysis of the basic mechanics involved in fluting (Appendix) suggests the following patterns:

1. differential shrinkage provides the compressive force which results in fluting at a given web tension,

2. the wavelength of the flutes is determined by the stiffness of the sheet when the critical failure load is exceeded (this is expected to be time/temperature dependent),

3. the wavelength and the degree of differential shrinkage determine the amplitude of the flutes.

Assuming that the inked layer serves as an equivalent heat and mass flux barrier regardless of the coating upon which it is applied, it may be logically inferred that differential shrinkage is governed primarily by coating/base sheet parameters. As the current study is limited to coating variables, the factors ex-

pected to contribute to fluting become coating stiffness/permeability and possibly thermal conductivity/thermal capacitance. Of these basic properties, the binder type is expected to most greatly influence stiffness while the pigment type may influence all relevant parameters.

Analyses of Binders

Because of the relative stability expected in basic sheet properties, the starch to latex series of experiments provides the most easily analyzed data set. It is presumed that the variations in binder cause significant changes in CD stiffness, but do not significantly impact the permeability or thermal properties of the coating. By extension, the amount of heat available to liberate internal web moisture and the rate at which the moisture may be expired should not be notably influenced by binder type. In turn, moisture loss in the unprinted region should remain constant for a given drying condition. Combining this argument with the aforementioned assumptions regarding the ink film (and lacking interactions), it is expected that differential shrinkage should remain constant by printing condition throughout the starch to latex series.

Experimental data largely support the arguments provided above. Shrinkage data available in Figure 12 indicate a fair consistency by drying condition, and an exceptionally flat trend on average. For this "fixed" condition in differential shrinkage, mechanics indicate that flute failure mode (wavelength) should be proportional to the fourth root of CD bending stiffness of the sheet at the temperature that corresponds to the critical failure load. The critical differential moisture change, in turn, is inversely proportional to the square root of CD elastic stiffness. Hence, the stiffer product should flute at lower differential moisture, and should produce longer wavelength (a smaller number of) flutes. The amplitude of the longest wavelength flutes must be highest to accommodate the fixed differential shrinkage condition.

Experimental data, again, support this argument. Comparison of the wavelength data of Figure 10 with CD elastic stiffness data (considered proportional to bending stiffness) in Figure 13 indicate that wavelength is roughly proportional to the square root of stiffness. The stiffness values in Figure 13 were extracted from the DeWildt (1999) report, and represent the CD product stiffnesses as measured at 100 degrees C. Flute amplitudes necessarily follow suit as the amplitude/wavelength ratio defined the initial argument.

A more rigorous interpretation of mechanics results would suggest that fluting wavelengths should be proportional to the fourth root of stiffness rather than the

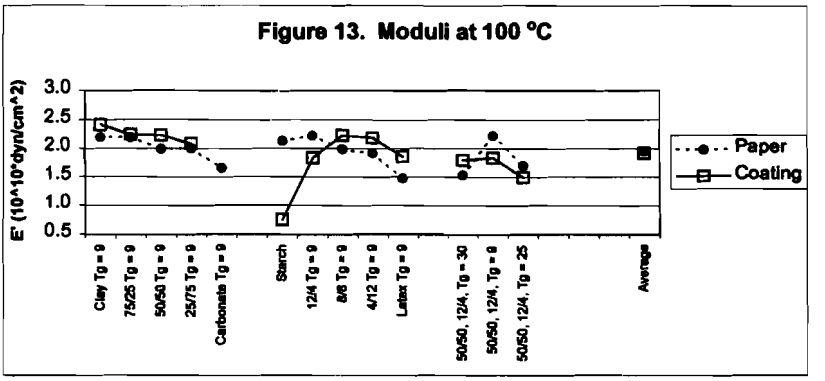

second. Errors introduced through simplifying the mechanics, coupled with the temperature sensitivity of stiffness values (DeWildt (1999)), may partially account for this discrepancy. A precisely coupled unsteady heat/mass transfer analyses with expanded mechanics is beyond the scope of the current endeavor.

Analyses of Pigments

Based on the results of the binder study, it seems logical to simplify fluting dynamics by assuming that product stiffness will proscribe flute wavelength and subsequently that differential shrinkage will define flute amplitude. Perhaps a more appropriate interpretation would be that binder stiffness will proscribe flute wavelength and subsequently that differential shrinkage will define flute amplitude. Current data suggest that pigment related stiffness enhancement does not affect flute wavelength. In either case, it appears that the pigment blend may govern the extent of differential shrinkage – and thereby influence flute amplitude.

In general terms, increasing the clay content of a coating is found to increase stiffness, decrease porosity, increase binder demand, and (arguably) increase thermal capacitance while decreasing thermal conductivity. Data in Figure 13 clearly illustrate the relationship between clay content and stiffness; however, this does not translate into the increased flute wavelengths evident in the binder study (Figure 9). All remaining trends associated with clay – decreased porosity, underbound condition (in this trial), increased thermal demand and decreased conduction – tend to decrease the rate at which water from the base sheet is evaporated through the coating. Fortunately, this trend is somewhat supported by the data (Figure 11, 12). Hence, as clay level is increased, shrinkage – and thereby flute amplitude – is decreased (Figure 7, 8).

The thermal analogy is drawn at this point, not because it is necessarily applicable, but because the trends anticipated by its inclusion cannot be distinguished directly based on available data. It is straightforward to equate porosity or permeability with evaporation rates; however, it is somewhat unlikely that the porosity effect dominates in this highly transient, low mass flux case. Drying rates on the web offset press during the current trials did not exceed 1#/hr*ft2. If the mass flux rate does not sufficiently exceed the low-pressure diffusivity limits for the coating, it is unlikely that coating serves as any substantive vapor barrier. It is specifically this diffusivity limit which causes blistering on press. Because no blistering was observed in white paper areas, and because evaporation rates exceeding the current maximum are typical in late phase drying in commercial coating operations, the inclusion of thermal variables is considered pertinent.

Figures 14 and 15 describe the influence of physical and thermal variables on drying in the imaged as well as the non-imaged areas. These figures are simplified and contain hypothetical values, and should be accepted for illustration purposes only. Figure 14 illustrates the influence of coating or ink porosity and/or thermal conductivity on transient drying. The drying rate curve is approximated in hyperbolic functions, and the variations in properties affect changes in the time constants. Similarly, Figure 15 illustrates the influence of coating or ink thermal capacitance for a fixed porosity (or conductivity). In this case, there is a "time delay" prior to moisture loss, but no subsequent change in time constant.

Figures 16 and 17 combine the physical and thermal processes into a crude model describing differential shrinkage dynamics. Figure 16 provides idealized curves representing trends associated with clay/carbonate coatings and ink application. As described above, the clay coating should release water more slowly than the carbonate coating. Similarly, the ink film serves as a capacitance increase (while volatiles are flashed) as well as a vapor barrier. Subtraction of such idealized curves provides a picture of the differential shrinkage changes indicative of products with varying pigment blends. The sensitivity analysis, which follows, makes use of this physical model.

Sensitivity to Press Operations

Figures 18 and 19 provide a good summary of the influence of coating variables on fluting, and also a good starting point for the discussion of press operations. The flute amplitude and wavelength data in Figures 18 and 19 represent the extreme conditions of maximum and minimum differential shrinkage on press. Data indicate that moving from a condition of maximum differential shrinkage on press to a minimum can reduce the amplitude of flutes more than 20% on average, while producing only a marginal change in wavelength. In both

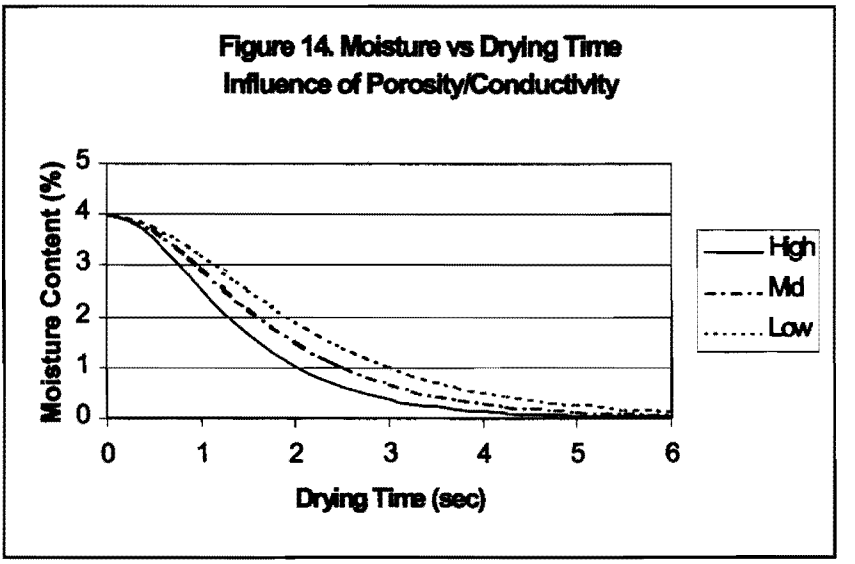
Figure 14. Moisture vs Drying Time
Influence of Porosity/Conductivity
Moisture Content (%)
0
1
2
3
4
5
0
1
2
3
4
5
6
Drying Time (sec)
High
Mid
Low

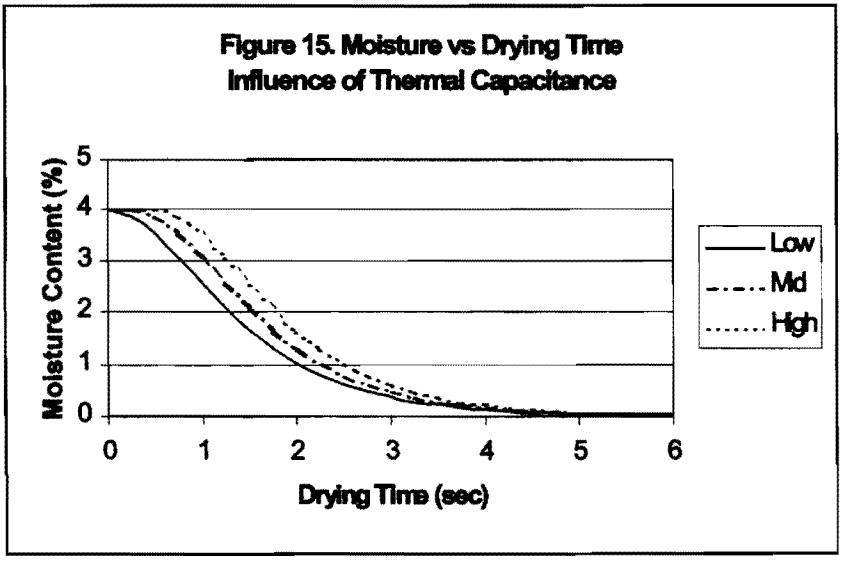
Figure 15. Moisture vs Drying Time
Influence of Thermal Capacitance
Moisture Content (%)
0
1
2
3
4
5
0
1
2
3
4
5
6
Drying Time (sec)
Low
Mid
High

Figure 16. Moisture vs Drying Time

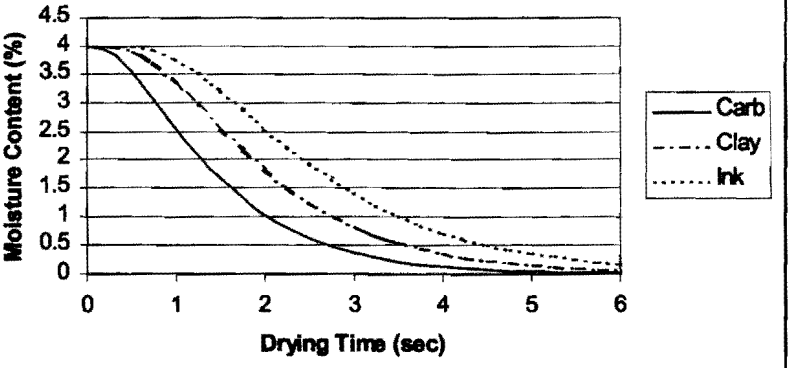

Figure 17. Differential Shrinkage

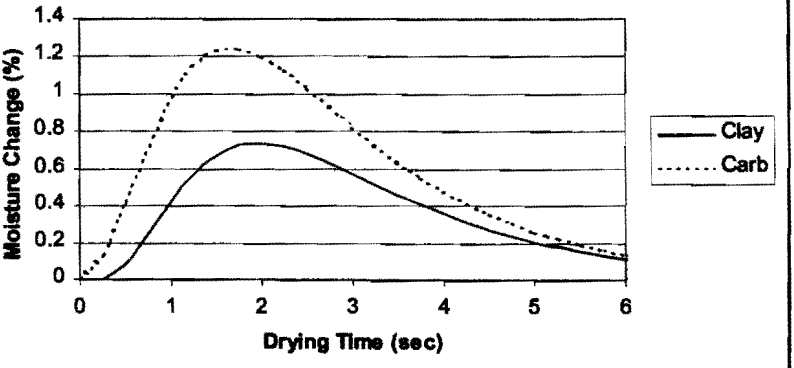

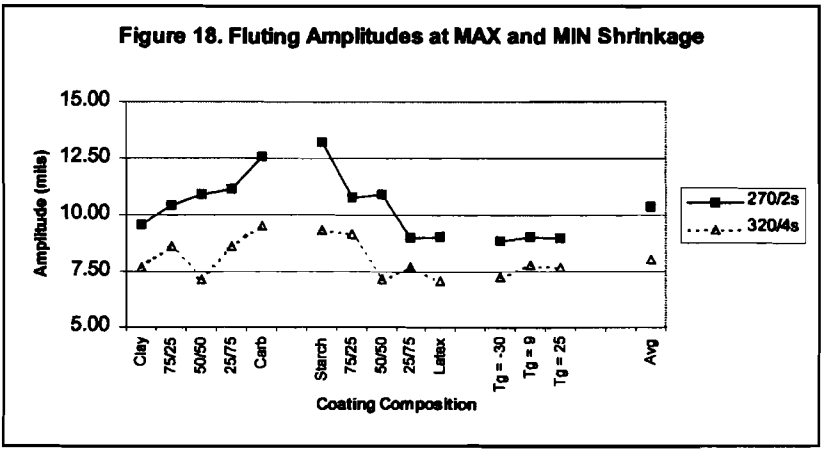

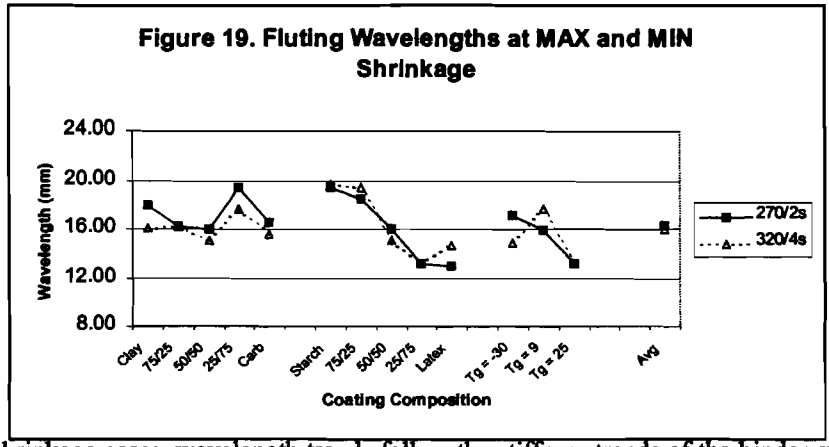

shrinkage cases, wavelength trends follow the stiffness trends of the binder system as provided in Figure 13 (the clay to carbonate series used one fixed binder system). Variations in amplitude are determined by (1) failure mode and (2) relative shrinkage. As shrinkage in the binder series is essentially constant for each press condition (a result of common pigmentation), the variations in amplitude simply reflect the variations in wavelength. Within the pigment series data, increasing carbonate leads to increasing differential shrinkage – which in turn increases flute amplitude at a fixed wavelength.

It was noted earlier that maximum differential shrinkage occurs at a maximum press speed and minimum oven temperature, while the minimum shrinkage occurs at a minimum press speed and a maximum oven temperature. This may at first seem counter-intuitive, but can be readily explained by reference to Figure

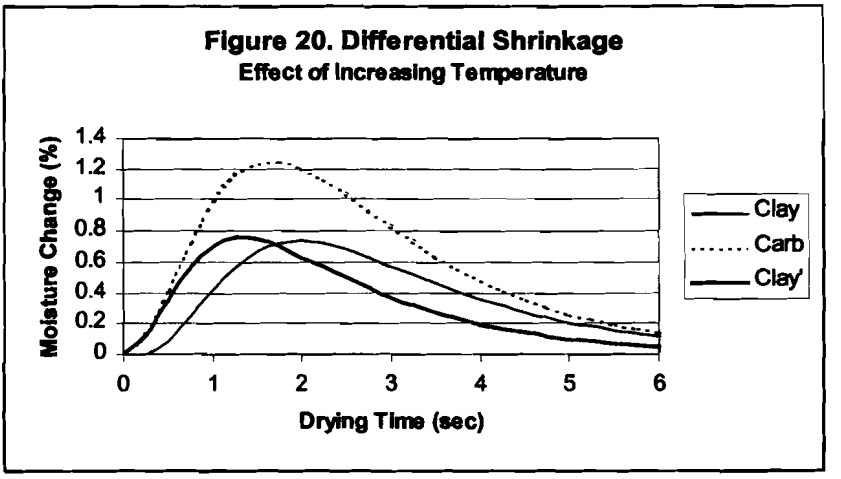

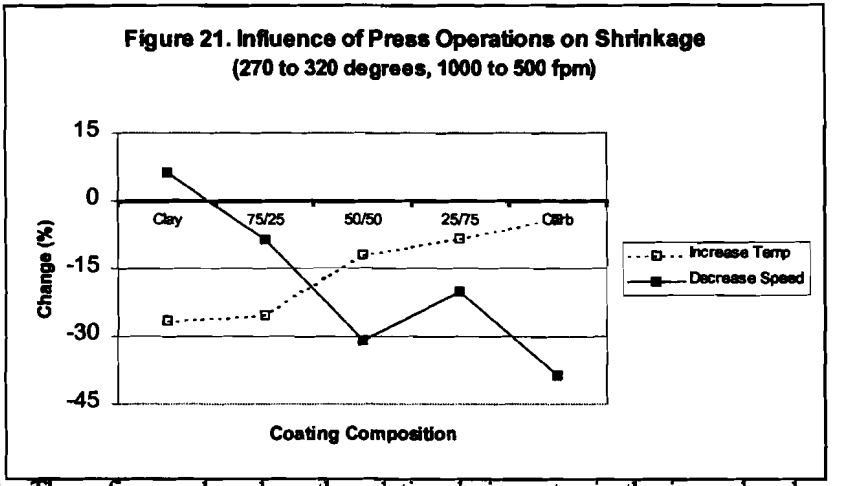

8. These figures show how the relative drying rates in the imaged and non-imaged regions may be combined to represent differential shrinkage as a function of coating pigmentation. Consider first the variable of drying time. It is evident in Figure 17 that as one extends the drying time from 2 seconds to 4 seconds, the amount of differential shrinkage becomes reduced for coatings of both pigment types. This is consistent with the field data, and reflects the fact that the moisture content has begun to level out in the non-imaged area, while substantive changes are occurring in the imaged area.

A change in oven temperature requires an adjustment of the idealized curves presented in Figure 17 to characterize the temperature influence. Figure 20 pro-

vides such an adjustment to the "clay" coating condition for reference. Increasing oven temperature will somewhat reduce the impact of thermal capacitance, shifting the curve slightly up and to the left as shown. In this fashion, a decrease in differential shrinkage with increasing temperature may be explained.

As stated above, Figures 7, 8, and 10 provide an illustration of the influence of physical and thermal variables on drying. They are, however, highly simplified and contain hypothetical values. Specific sensitivity trends, therefore, are examined based solely on the experimental data. Figure 21 presents shrinkage sensitivities to press conditions for the pigment series data.

It is evident from the data in Figure 21 that the path taken to reduce shrinkage may be expected to have a variable return based on the coating composition. Current findings indicate that high clay containing coatings are most sensitive to press oven temperature. Conversely, high carbonate containing coatings are most sensitive to heating duration, or press speed.

In closing, it should be noted that the specific findings regarding press operational sensitivities may be specific to the conditions under examination in the study. It is reasonable to assume that a commercial press laying down a variable image may be operating at a speed such that decreasing speed does not improve fluting, or at a temperature such that increasing temperature does not improve fluting. In addition, the current analysis has been written with the expectation that increasing amplitude and frequency of flutes is undesirable.

Acknowledgements

We wish to thank Blake Davis and Bill Mallory of Mead Central Research for their work in developing the test procedures for analyzing flute frequency and amplitude, and in carrying out the measurements on the samples in this study.

References

DeWildt, D.
1999 "Paper Coating Components Dynamic Mechanical Spectroscopy (DMS) Testing," Dow report to MCR (Mead Fluting Project), December 1999.

Hirabayashi, T., Fujiwara, S., and Fukui, T.
1998 "Factors of fluting of coated paper in web-offset printing," 1998 Pan-Pacific and International Printing and Graphic Arts Conference (Pulp and Paper Technical Association of Canada) 1998

MacPhee, J., Bellini, V., Blom, B., Cieri, A., Pinzone, V., and Potter, R.
2000 "The effects of certain variables on fluting in heatset web offset printing," Web Offset Association, 100 Daingerfield Road, Alexandria, Virginia, 22314-2888 USA.

Mochizuki, S., Aoyama, J.
1981 "Effects of fast ink drying conditions on multi-colored moving web-(I)", TAGA Proceedings, 1981, PP 43-55

APPENDIX

We hypothesize that differential moisture changes lead to differential shrinkage in the imaged and non-imaged areas during drying, and that this creates compressive stresses in the inked area, which in turn leads to fluting of the web. In order to quantify this assertion, a stress and stability analysis of a model problem was conducted. A schematic of the model problem is shown in Figure A1. This model corresponds closely to the laboratory fluter at Mead Central Research and in a loose way relates to the web in a dryer of an offset printer.

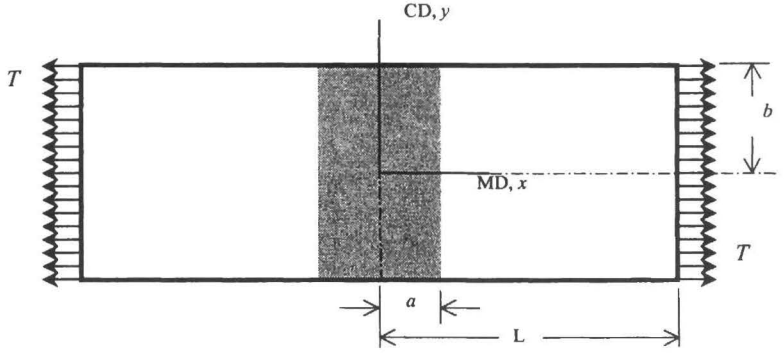

Figure A1. Model web for fluting analysis. The shaded area represents the inked region of the web. A tension, T, is applied in the MD. The web width is b, the web length is L, and the extent of the inked area is a.

For the analysis, it was assumed that the moisture change in the inked area, m, is less than the moisture change in the non-inked area, $\widetilde{m}$. The material behavior of the web was taken to be linear elastic and orthotropic and including hygroexpansion. An analytic solution of the in-plane stresses in the inked region was developed. An example of the stress distribution in ¼ the inked region is given in Figure A2. Note that the CD stresses are compressive in the inked domain. Further analysis showed that the CD stresses are tensile directly outside the inked area. A finite element analysis of the model problem verified the analytic results.

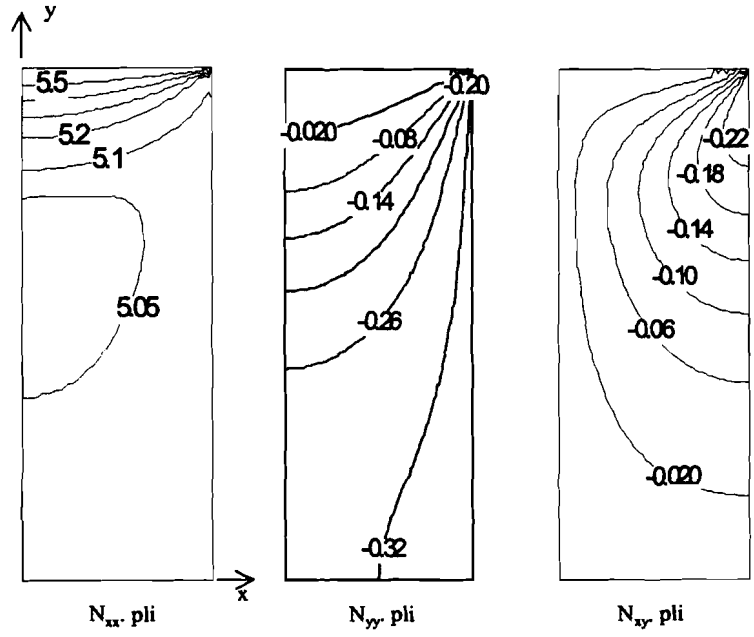

Figure A2. Stress distribution in inked region. N_{xx} is the MD stress, N_{yy} is the CD stress, and N_{xy} is the in-plane shear stress. ($E_{11}t$= 900 pli., $E_{22}t$= 400 pli, $G_{12}t$= 217 pli, ν_{12}= 0.45, β= 0.001 1/%m, L= 9 in., a=1.5 in., t=0.004 in , b=4.25 in., m = -2.5%, $\tilde{m}$ = -0.8%, and T=5.1 pli.)

A linear buckling analysis of the model problem was conducted to determine the critical moisture change that induces buckling, the extent of the waves into the un-inked region, and the wavelength of the wrinkles. The critical moisture change was determined by minimizing the potential energy for the flute shape given below.

$$w(x,y) = \begin{cases} A[1+\cos(\pi x/c)]\sin(2\pi y/d) & 0 \le x \le c \\ 0 & c \le x \le L \end{cases}$$

In this expression, d is the wavelength of the flutes, and c is the extent of the flutes in the MD direction. The important aspect in the stability analysis is that we have allowed the extent of the flutes to vary from the inked area c=a, to the full web length c=L. If c is determined to be less than L the flutes are considered localized. The predicted wavelength of the resulting flutes is given by

$$d = \frac{2\sqrt[4]{3}\,c}{\sqrt[4]{\frac{D_{11}}{D_{22}} + \frac{Tc^2}{\pi^2 D_{22}}}}$$

Where the value of c must be determined as the value that minimizes the critical moisture difference. The equation that determines the critical moisture difference is quite complex, but for the case where the web tension is fairly large the results can be approximated by

$$(\tilde{m} - m)_{cr} = \frac{1.2}{K\beta_{22}}\sqrt{\frac{T}{C_{22}}}\,\frac{t}{a},$$

$$d = 7.1\sqrt[4]{\frac{D_{22}a^2}{T}}, \quad c = 2.3a \quad .05 < a/L < .45$$

where K is a stress intensity factor to account for the nonuniform distribution of CD stresses in the inked domain, $C_{22} = \frac{E_{22}t}{(1-\nu_{12}\nu_{21})}$ is the integrated CD plane stress stiffness, and $D_{22} = \frac{E_{22}t^3}{12(1-\nu_{12}\nu_{21})}$ is the CD bending stiffness. Note that the analysis does reveal that the flutes will be localized to the region near the inked area, but extend past the flutes. This was verified by the results of a laboratory fluting trial conducted at Mead Central Research. The material and geometric properties measured for the fluting tests are the same as those given in the caption of Figure A2. The applied tension was varied and resulting flute wavelengths were measured. Figure A3 shows a comparison of the prediction versus experimental measurements. The fit is fairly good except at the extreme levels of the tension. All the values for the predictions were taken from experimental data and no fitting was used for the predictions shown in Figure A3.

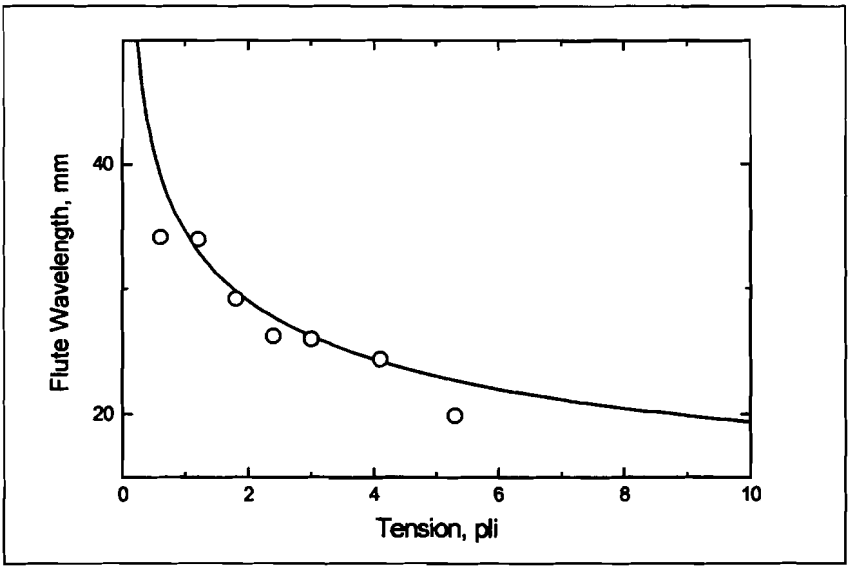

Figure A3. Comparison of experimental results (o) to predictions (-).

The prediction for the critical moisture difference to induce buckling is given as $(\tilde{m} - m)_{cr} = 0.5\%$ for T=5 pli, a=1.5 in, t=0.004 in., C_{22} =400 pli, K=0.68, and β_{22} = .001/%mc. This is sufficiently below the measured value of 1.7% such that significant fluting should be observed.

In summary, the important findings of the analysis are as follows:

- Differential moisture content changes observed in the inked and non-inked regions are sufficient to cause fluting.
- Fluting is localized near the inked region due to the tensile CD stresses in the adjoining non-inked regions.
- Flute wavelength will be a function of web tension, the MD length of inked area, and CD bending stiffness of the sheet.
- The amplitude of the flutes will depend on the magnitude of differential moisture content, the coefficient of hygroexpansion, and the flute-wavelength.